A novel naphthyridine carboxamide provides evidence for discordant resistance between mechanistically identical inhibitors of HIV-1 integrase

Authors:

Daria J. Hazuda[#1], Neville J. Anthony[#2], Robert P. Gomez[2], Samson M. Jolly[2], John S. Wai[2], Linghang Zhuang[2], Thorsten E. Fisher[2], Mark Embrey[2], James P. Guare Jr[2], Melissa S. Egbertson[2], Joseph P. Vacca[2], Joel R. Huff[2], Peter J. Felock[1], Marc V. Witmer[1], Kara A. Stillmock[1], Robert Danovich[1], Jay Grobler[1], Michael D. Miller[1], Amy S. Espeseth[1], Lixia Jin[3], I-Wu Chen[3], Jiunn H. Lin[3], Kelem Kassahun[3], Joan D. Ellis[3], Bradley K. Wong[3], Wei Xu[3], Paul G. Pearson[3], William A. Schleif[4], Emilio Emini[4], M. Katharine Holloway[5], and Steven D. Young[2].

 # To whom correspondence should be addressed.
E-mail neville_anthony@merck.com **and** daria_hazuda@merck.com
Telephone 215-652-7204
Fax 215-652-0994

Departments of Biological Chemistry[1], Medicinal Chemistry[2], Drug Metabolism and Pharmaceutical Research[3], Vaccine Research[4], and Molecular Systems[5]
Merck Research Laboratories, P.O. Box 4. West Point, PA 19486. USA.

Abstract

The increasing incidence of resistance to current HIV-1 therapy underscores the need to develop antiretroviral agents with new mechanisms of action. Integrase, one of three viral enzymes essential for HIV-1 replication, presents an important yet unexploited opportunity for drug development. We describe here the identification and characterization of L-870,810, a small molecule inhibitor of HIV-1 integrase with potent antiviral activity in cell culture and good pharmacokinetic properties. L-870,810 is a structurally novel inhibitor with an 8-hydroxy-(1,6)-naphthyridine-7-carboxamide pharmacophore. The compound inhibits HIV-1 integrase mediated strand transfer and its antiviral activity *in vitro* is a direct consequence of this ascribed effect on integration. L-870,810 is mechanistically identical to previously described inhibitors from the diketo acid series, however, viruses selected for resistance to L-870,810 contain mutations (integrase residues 72, 121 and 125) which uniquely confer resistance to the napthyridine. Conversely, mutations associated with resistance to the diketo acid do not engender napthyridine resistance. Importantly, the mutations associated with resistance to each of these inhibitors map to distinct regions within the integrase active site. We therefore propose a model of the two inhibitors that is consistent with this observation and suggests specific interactions with discrete binding sites for each ligand. These studies provide a structural basis and rationale for developing novel integrase inhibitors with the potential for unique and non-overlapping resistance profiles.

Introduction

Agents for the treatment of HIV-1 infection target two of the three virally encoded enzymes and belong to three mechanistic classes known as nucleoside reverse transcriptase (NRTI), non-nucleoside reverse transcriptase (NNRTI) and protease (PI) inhibitors. Although treatment regimens using combinations of these agents have significantly reduced AIDS related morbidity and mortality, it is currently estimated that 78% of treatment naive patients harbor viruses that have evolved resistance to at least one of these drug classes. [1,2] The emergence of HIV-1 strains resistant to reverse transcriptase and protease inhibitors highlights the need to develop antiviral agents with novel mechanisms of action.

Integrase [3,4] , one of the three virally-encoded enzymes required for HIV-1 replication, catalyses the integration of viral DNA into the genome of the host cell. The integration reaction requires three discrete steps: assembly of a stable preintegration complex at the termini of the viral DNA and two sequential transesterification reactions. In the first reaction, 3' end-processing, endonucleolytic cleavage of the two 3' nucleotides at each DNA end generates 3' hydroxyl groups that function as nucleophiles in the second reaction. The strand breakage of the cellular DNA and concomitant covalent linkage with the viral DNA is a consequence of the second transesterification reaction, strand transfer.

The discovery of a series of diketo-acid containing HIV-1 integrase inhibitors,[5, 6] exemplified by L-731,988 (**1**), (Figure 1) that prevent integration and viral replication in cell culture, provided the first proof of concept for HIV-1 integrase inhibitors as antiviral agents. These compounds were shown to act specifically as inhibitors of the integrase strand transfer reaction by virtue of their ability to bind selectively to the enzyme complexed with the viral (or donor) DNA and compete with the host (or target) DNA substrate. [7,8] The critical diketo carboxylate pharmacophore interacts with critical divalent metal ions in the active site[8] and mutations that engender resistance to these prototype inhibitors[5, 9] as well as closely related analogs map to the integrase active site proximal to residues which coordinate divalent metals (D66, D116 and E152). These observations are consistent with the proposed mechanism of action and provide further validation for integrase as the target of their antiviral effect.[5] Subsequently, a series of rational structure activity relationships (SAR) have afforded a variety of such analogs with improved activities.[6, 10, 11, 12, 13]

Herein we describe the identification and characterization of a novel inhibitor, L-870,810, which contains a structurally distinct 8-hydroxy-(1,6)-naphthyridine-7-carboxamide pharmacophore. L-870,810 has a mechanism of action that is indistinguishable from the diketo-acids, displays potent antiviral activity and has pharmacokinetic properties suitable for clinical development. Although both the biochemical and antiviral activities of L-870,810 are analogous to the diketo acids, we provide evidence that these inhibitors exhibit discordant sensitivity to resistance mutations. Exploration of the structural basis for this unexpected result provides new insights into this novel class of antiviral agents and suggests an approach to the development of integrase inhibitors with unique resistance profiles.

Materials and Methods.

Preparation of L-870,810 and analogs. The synthesis of L-870,810 and analogs has been described.[14] The compound may be prepared as an anhydrous white powder or as a yellow anhydrous crystalline sodium salt, m.p. 338°C. The ionization constant of the phenol group was determined by spectrophotometric titration in aqueous methanol. The aqueous pKa was estimated to be 7.3 by extrapolation to zero organic solvent content. Additionally, the octanol: water partition coefficient, log P, was determined by HPLC analysis to be 2.09.

HIV-1 Integrase Assays.

Strand Transfer Assay

HIV-1 and SIV integrase were purified as described. [15] RSV integrase was the generous gift of Dr. Duane Grandgenett, St. Louis University. Integrase mediated strand transfer activity was determined as described previously.[12] Biotinylated donor DNA was immobilized onto streptavidin coated microtiter plates. Integrase was assembled onto the donor in (20 mM Hepes, pH 7.6, 40 mM NaCl, 5 mM 2-mercaptoethanol, 50 μg/ml bovine serum albumin) with 25 mM $MnCl_2$. The complexes were washed prior to the addition of a target substrate 3' end-labeled with fluorescein isothiocyanate (FITC). Strand transfer reactions were performed in 2.5 mM $MgCl_2$ using 0.5 or 5 nM target DNA. FITC labeled products were detected using an anti-FITC antibody conjugated with alkaline phosphatase (Boehringer Mannheim) and a chemiluminescence substrate

(Sapphire II, Tropix). Inhibition of strand transfer was evaluated by adding compounds immediately prior to the addition of target substrate.

Competitive binding. ^{3}H-L-731,988 **(1)** (4-[1-(4-fluorobenzyl)pyrrole-2-yl-2,4-diketobutanoic acid) was prepared by catalytic tritiation of the corresponding iodopyrrole. Competition binding experiments were performed as described. [8]

HIV-1 replication a(Spread) ssays. Assays were performed in MT-4 human T-lymphoid cells or primary PBMCs as described.[16] Cells were infected en masse at low multiplicity (0.01). HIV-1 replication was assessed by p24 core antigen ELISA. Single cycle infection assays were performed as previously described.[5]

Measurement of HIV-1 DNA synthesis, integration and 2-LTR circles.
Viral DNA synthesis and 2-LTR circles were evaluated using quantitative PCR (Taqman).[5] SupT1 cells were preincubated in the presence or absence of 10 μM L-731,988, 1 μM L-870,810, or 10 μM L-697,661 (NNRTI) for 1 h at 37°C and then infected with HIV-1 by co-culture with the chronic producer line Molt-IIIB. Low molecular weight DNA was harvested at various times to quantify each HIV-1 product. Late reverse transcripts were amplified using primers and probes specific for DNA made after the second template switch of reverse transcription. Quantification of reverse transcription products at six hours post-infection was performed relative to standards using the HIV-1 proviral plasmid pNL4-3. HIV-1 2-LTR circles were evaluated at 24 hours post-infection using a 2-LTR primer/probe set and standards generated using a cloned DNA fragment corresponding to a 2-LTR circle junction of HIV-1 DNA (154 bp from the U5 region, 408 bp from the U3 region). To determine the fraction of total HIV-1 DNA molecules in the 2-LTR circular form, the number of 2-LTR circles was divided by the number of total HIV-1 DNA molecules. Extracts were normalized for overall DNA recovery by assessing mitochondrial DNA using a primer/probe set for cytochrome oxidase.

Quantitative PCR was also used to evaluation integration in the presence or absence of inhibitors at 24 hours post-infection by assessing integration events that occur near the repetitive genomic DNA element Alu using an Alu-LTR primer/probe set.[17] To quantify relative integration events, genomic DNA from infected control cultures was serially

diluted with a constant amount of DNA from uninfected cells to establish a standard curve.

Animal Pharmacokinetic Studies. The pharmacokinetic parameters of L-870,810 were determined in rats, dogs and rhesus macaques. Three male Sprague-Dawley rats received an intravenous (i.v.) dose of 2 $mgkg^{-1}$ as a solution in DMSO via an indwelling cannula implanted in the jugular vein. After an overnight fast, 3 additional animals received an oral dose of 10 mg kg^{-1} as a suspension in 1% aqueous methylcellulose. The absolute oral bioavailability was determined by comparing the mean area under the plasma concentration /time curve (AUC) obtained from each group.

Similar procedures were used to evaluate pharmacokinetic parameters in dogs and rhesus macaques. Four animals per group received i.v. and oral doses in a cross over fashion. Following an overnight fast, each animal received an oral dose of L-870,810 at 1 mg kg^{-1} as a suspension in 0.5% aqueous methylcellulose. After a washout period, the animal received an i.v. dose of L-870,810 (1 mg kg^{-1}) as a solution in DMSO (0.1 mg kg^{-1}). Absolute oral bioavailability was determined by comparing the AUC after oral administration with that obtained from the i.v. dose. L-870,810 plasma concentrations were determined by LCMS analysis.

Molecular Modeling Fifty conformers of L-870,810 and the diketo acid (**2**) were generated using a distance geometry method[18] and subsequently energy-minimized using the MMFF force field[19] with a 2r dielectric constant. A low energy conformer of each inhibitor was selected to illustrate the proposed overlays of the metal chelating pharmacophore elements as depicted in Figure 5. The selection was supported by strong agreement between the low energy conformer of L-870,810 and a small-molecule X-ray structure (data not shown). The low energy conformers were then manually docked into the active site of the C monomer of the 1BL3 HIV-1 Integrase crystal structure.[20] The keto and enol oxygens of **2** and the keto and 8-hydroxy oxygens of L-870,810 were aligned with two of the Mg coordinated water molecules (11 and 149) in the crystal structure. Additionally, the acid O in **2** and N1 of the L870,810 naphthyridine ring were positioned to interact with a putative second Mg positioned between D64 and E152. The positions of the pendant aromatic groups were modified slightly to optimize contacts with the active site surface.

Results

L-870,810 is a structurally novel inhibitor of integrase mediated strand transfer

We previously reported the discovery of a series of diketo-acid containing HIV-1 integrase inhibitors,[5,6] exemplified by L-731,988 (**1**) and the potent analog (**2**) (Figure 1). These compounds bind selectively to the enzyme/viral DNA complex and act specifically as inhibitors of the strand transfer reaction. Structure activity relationships for the diketo-acid inhibitors have been discerned and it was found that the carboxylate could be mimicked by a suitable heterocycle bearing a lone pair donor atom [21, 22], affording diketone based inhibitors such as (**3**). Although the 1,3 diketone motif common to these compounds is a key element of the pharmacophore required for inhibitory activity, the chemical reactivity of this functionality provoked efforts to reduce it's electrophilicity. This resulted in the 1,6-naphthyridine ketone,[12] (**4**) in which one of the enolizable ketones is replaced with a phenolic hydroxyl group. The remaining phenyl ketone was then replaced with a 4-fluorobenzyl carboxamide moiety. Further refinement with respect to *in vitro* antiviral potency and pharmacologic properties ultimately identified a 6-membered cyclic sulfonamide as an optimal substituent at the 5-position of the 8-hydroxy-(1,6)-naphthyridine carboxamide core providing the inhibitor L-870,810.[14]

L-870,810 is a potent inhibitor of HIV-1 integrase and the highly homologous enzyme from SIV but is inactive against the more distantly related RSV integrase (IC_{50} > 50 μM) (data not shown). Like the diketo acids, L-870,810 is a selective inhibitor of HIV-1 integrase mediated strand transfer. When assayed using purified recombinant HIV-1 integrase, L-870,810 inhibits strand transfer with apparent IC_{50}'s of 8 or 15 nM using 0.5 nM and 5 nM target DNA, respectively. L-870,810 exhibits reduced activity with respect to assembly and 3' end processing (IC_{50}'s of 85 and 250 nM in 0.5 and 5 nM target DNA). The preferential inhibition of strand transfer and the sensitivity of L-870,810 to the concentration of target substrate are consistent with previous studies[7] that suggest these inhibitors bind to the target DNA site of the integration complex. In competition binding experiments, L-870,810 displaces radiolabeled L-731,988 (**1**) from the integrase donor complex with a K_i of 3 nM (data not shown) indicating that these inhibitors bind to the assembled DNA complex within the same or overlapping regions of the active site.

L-870,810 is an orally available inhibitor which exhibits broad spectrum activity against wild type and multi-drug resistant HIV-1, HIV-2 and SIV

The antiviral activity of L-870,810 was profiled in viral replication assays using different cell types and a variety of M- and T-tropic isolates of HIV-1. In the presence of 10% FBS or 50% normal human serum, the compound inhibits the replication of the laboratory adapted HIV-1 isolate H9/IIIB in MT-4 T lymphoid cells with mean CIC_{95}'s of 15 nM and 100 nM, respectively. L-870,810 also inhibits HIV-1 clinical isolates and exhibits comparable activity against non-syncytia (NSI) and syncytia (SI) viruses from clades A, B, C, D and F. As expected for a novel mechanism, L-870,810 is active against multi-drug resistant viruses such as MDRC4 (IC_{50}'s of 4 nM), which has multiple mutations in reverse transcriptase and protease and exhibits 5 fold or greater resistance to most NRTIs, NNRTIs and PIs (N. Parkin, personal communication). Consistent with the observation that L-870,810 inhibits SIV integrase, L-870,810 inhibits the replication of both SIV (CIC_{95} of 7-15 nM in 10% FBS) and the highly homologous virus HIV-2 (CIC_{95} of 8 nM in10% FBS). The potential for efficacy in HIV-2 infection is of interest as most current antiretroviral agents are poorly active against this human pathogen.

The pharmacokinetic parameters for L-870,810 were measured in three preclinical species. L-870,810 is characterized by low plasma clearance of 2.8, 2.0 and 6.6 mL/min/kg in rats, dogs and rhesus macaques respectively. Biphasic pharmacokinetics were observed in rats and macaques with $T_{1/2}$ of 1.13 and 1.4 hours and terminal half lives $T_{1/2}$ of 14.0 and 9.6 hours respectively. In dogs the elimination is monophasic with a half life of 2.3 hours. L-870,810 has an oral bioavailability of 41%, 24% and 51%, in rats, dogs and rhesus macaques respectively. Importantly, drug concentrations that exceed the CIC_{95} of 100 nM are observed for approximately 12 hours following a 5 mg kg^{-1} oral dose to rats and dogs (Figure 2).

The antiviral activity of L-870,810 is a direct consequence of its effect on integration.

The mechanism of action of L-870,810 on HIV-1 replication was evaluated by assessing DNA synthesis and integration in infected cells using quantitative PCR. SupT1 cells were acutely infected by co-culturing the cells with the HIV-1 chronic producer Molt-IIIB cells in the presence or absence of L-870,810, the diketo-acid L-731,988, and the NNRTI, L-697,661.[23] HIV-1 specific products were quantified and normalized relative to mitochondrial DNA. Neither L-870,810 nor the diketo-acid affect reverse transcription at concentrations ten-fold greater than that required to inhibit replication (data not shown). In contrast, both L-870,810 and the diketo-acid reduce the

integrated HIV-1 DNA to undetectable levels and increase 2-LTR circles; at 24 hr post infection, a 5.9 fold increase in 2-LTR circles was observed with L-870,810 (Figure 3). Neither integrated HIV-1 DNA or unintegrated 2-LTR circle DNAs were detected in the presence of the NNRTI. As shown for the diketo acids, the absence of integration products and the accumulation of 2-LTR circles provide evidence that the antiviral activity of L-870,810 is a direct consequence of its effect on integration.

L-870,810 resistant variants contain unique active site mutations and are not cross resistant to diketo acids

Like the diketo acid inhibitors, serial passage of HIV-1 in cell culture in the presence of L-870,810 selects for viruses that exhibit reduced susceptibility to the inhibitor and accumulate mutations in integrase. Population sequencing of the integrase coding region in multiple clones intermittently during selection with L-870,810 identified mutations that were acquired sequentially over several months: F121Y/T125K (six months), V72I/F121Y/T125K and V72I/F121Y/T125K/V151I (3/8 and 5/8 clones, respectively after 9 months). Although the L-870,810 mutations map within the integrase active site (see below) they are distinct from mutations observed with diketo acid analogs (eg., L-731,988 and L-708,906: T66I/S153Y, T66I/M154I[5] or **(2)** : T66I/S153Y and N155S, Witmer and Hazuda, unpublished).

A panel of viruses containing the diketo acid resistance mutations and L-870,810 mutations were constructed and evaluated for their susceptibility to L-870,810 and diketo acid **(2)** (Table 1). Viruses containing mutations selected by L-870,810 were four to one hundred-fold less sensitive to the inhibitor and resistance was enhanced with the addition of those mutations accumulated during selection. In every case, however, the L-870,810 resistant viruses remain sensitive to the diketo acid. Conversely, with the exception of N155S, the mutations selected with the diketo acid engender resistance to this inhibitor without affecting L-870,810 activity. Similarly discordant profiles were also observed with other diketo acid and naphthyridine analogs (data not shown).

The lack of overt cross resistance observed with the 8-hydroxy-(1,6)-naphthyridine carboxamides and diketo acids while surprising, is entirely consistent with selection of distinct resistance mutations. Mapping of these residues within the integrase crystal structure is shown in Figure 4. The active site residues (D64, D116 and E152 in yellow) are believed to coordinate the two magnesium ions which interact with the pharmacophores in these inhibitors. Both the diketo acid and L-870,810 mutations

surround the metal binding site consistent with the proposed mechanism of action. However, residues that are uniquely associated with either L-870,810 (magenta) or diketo acid (green) resistance cluster on distinct sides of the active site. Interestingly, N155, the only mutant with significant cross resistance, points directly into the active site and hydrogen bonds with the critical metal binding residue D116. A mutation of N155 could directly affect the interaction with both inhibitors by disrupting metal binding. This is consistent with the observation that the N155S mutant is impaired for enzymatic function and viral replication (<30% wild type HIV in infectivity assays, data not shown).

The majority of mutations are uniquely associated with resistance to one inhibitor and map more distal to the metal binding residues (Figure 4). Moreover, the mutations associated with each inhibitor map to discrete sites in the crystal structure indicating their respective interactions extend beyond the metal binding center in separate directions within the active site and suggest the two compounds may bind in opposite orientations. Assuming that the diketo acid and 8-hydroxy-(1,6)-naphthyridine carboxamide moieties form a metal chelating pharmacophore, low-energy models of L-870,810 and diketo acid **(2)** can be overlaid in a 'forward' or 'reverse' direction, as illustrated in Figure 5A and B. In the 'reverse' overlay, there is overlap of the metal binding pharmacophores but not of the pendant substituents. The two molecules were docked in the active site such that the two phamacophores could engage magnesium ions bound between D64 and D116, and between D116 and E152, respectively (Figure 5C). In this model the overlay which places the two inhibitors in the reverse orientation is the most consistent with both a similar binding mode for the two inhibitors and a divergent pattern of resistant mutations.

Discussion

We have described the identification and characterization of L-870,810, a novel orally bioavailable inhibitor of integrase, which inhibits HIV-1 replication through its effect on viral integration. Based upon the compound's potent activity against diverse clinical isolates and drug resistant HIV-1 *in vitro* and promising preclinical pharmacokinetic profile, L-870,810 exemplifies a class of agents that target HIV-1 integrase with the potential for clinical utility. L-870,810 is also the prototype of a novel structural class of 8-hydroxy-1,6-napthyridine-7-carboxamides which provide a new pharmacophore for inhibitor design. Like previously described diketo acids, the 8-hydroxy-1,6-napthyridine-7-carboxamides selectively inhibit integrase mediated strand transfer[5,7]. Although these

inhibitors are mechanistically indistinguishable, we have shown that distinct resistance profiles can be obtained with homologous napthyridine and diketo acid analogs providing the proof of concept and rationale for designing integrase inhibitors with the potential for unique and non-overlapping resistance.

We have explored the molecular basis for the discordant resistance profiles of the naphthyridine and the diketo acid and suggest that while the two pharmacophores engage divalent metals within the integrase active site they may bind in opposite orientations. The 8-hydroxy-(1,6)-naphthyridine carboxamide conserves the spatial orientation of the chelating moieties in the diketo acid that have previously been shown to be essential for activity and this spacing is consistent with the distance between the two active site metals observed in the crystal structure of ASV integrase and other divalent metal dependent phosphotransferases.[8] While in some cases resistance may be mediated by mutations which can affect the metal coordinating residues in integrase and alter the geometry of the active site (e.g., the mutations 155 or 66), other residues associated with resistance are more distal to the metal binding site. The observation that the latter mutations can be selective for different inhibitors and map to distinct regions within the integrase active site suggests these inhibitor/enzyme interactions may extend beyond the pharmacophore in different directions.

Molecular modeling studies of low-energy conformers indicate the essential elements of the diketo acid and 8-hydroxy-(1,6)-naphthyridine-7-carboxamide pharmacophores can align equally well in either direction. However, the distinct resistance profiles of the compounds would be most consistent with the two pharmacophores binding in reverse orientations, fixing the respective substituents in opposing directions. The proposed model which places the two inhibitors in the reverse orientation is also consistent with the SAR observed for structurally related analogs in both inhibitor series (data not shown). The precise orientation of each inhibitor in the active site may therefore be the result of establishing the most favorable interactions of the specific substituents and accommodating the increased rigidity and bulkiness of the napthyridine relative to the more flexible diketo acid. The suggestion that affinity and specificity is driven by the pendant groups in these molecules is consistent with studies which have shown that diketone analogs which lack a carboxylate bind with relatively high affinity even though they do not inhibit integrase enzymatic activity[8] and the observation that pharmacophores in which substituents are extended in both directions can exhibit enhanced affinity (data not shown). In addition, although the respective SAR

is quite distinct, the adaptable diketo acid pharmacophore can be exploited as a template for inhibitors of a variety of divalent metal dependent phosphotransferases, such as HIV-1 RNase H[24] and HCV polymerase[25]. In contrast, the more rigid napthyridines appear to be particularly restricted to integrase (S. Young and D. Hazuda, unpublished). These observations are interesting in the context of published molecular dynamics simulations with a diketo tetrazole inhibitor, 5CITEP, that have suggested the potential for two conformations of this flexible inhibitor in the docked structure and two possible ligand binding regions adjacent to the integrase active site[26].

High affinity interaction of strand transfer inhibitors with integrase requires a specific DNA bound conformation[7] and obtaining a structure of the inhibitor bound integrase complex with DNA has not been achieved to date. While crystal structures of various integrase sub-domains have been published[20,27,28], the active site has proven highly flexible and the structure in the region most relevant for the interaction with these inhibitors is not precisely known. The suggestion that the active site adopts a unique conformation upon binding the DNA is consistent with the observation that in the proposed model the residues associated with resistance are located proximal to the respective inhibitors but do not make direct contact with each molecule. The lack of structural information with sufficient detail to facilitate the design of integrase inhibitors therefore continues to present a substantial challenge. Although we do not have accurate structural information, resistance profiling and the association of selected mutations with specific inhibitors provide valuable insights into how these inhibitors may interact within the integrase active site. The observation that different classes of integrase inhibitors both select for and are influenced by unique mutations indicates that high affinity molecules can be obtained wherein the critical interactions are established in different regions of the active site and suggests a molecular basis for developing novel integrase inhibitors with discordant resistance profiles.

Acknowledgments: The authors would like to thank C. Petropolous and N. Parkin for assistance in evaluating multi-drug resistant variants.

Figure Legends

Figure 1: Evolution of L-870,810 from the diketo-acids, L-731,988 **(1)**[5] and **(2)**[6].

Figure 2: Pharmokinetic profile of L-870,810 after intravenous and oral administration to rats and dogs.

Figure 3: L-870,810 inhibits integration and increases the number of 2-LTR circles in HIV-1 infected cells.
Integration products and 2-LTR circles in HIV-1 infected cells were evaluated in the presence or absence of L-870,810, a diketo acid L-731,988 and an NNRTI by RT-PCR. All samples were standardized to a mitochondrial DNA control and quantified relative to known standards as described.

Figure 4: Mutations associated with diketo acid and L-870,810 resistance map to the integrase active site.
The three dimensional structure[20] of the HIV-1 integrase active site is depicted as a white α-carbon pipe. The active site residues (D64, D116 and E152), highlighted in yellow, are believed to coordinate two divalent metals, although only one, shown as a purple ball, is evident in this structure. Residues associated with resistance to diketo acids **(1)** and **(2)** are shown in green; those associated with resistance to L-870,810 are shown in magenta.

Figure 5: Modeling of the diketo acid and 8-hydroxy-(1,6)-naphthyridine-7- carboxamide pharmacophores suggest two potential binding modes.
Low energy conformers of diketo acid **(2)** (green) and L-870,810 (magenta) with the pharmacophores aligned in the "forward" and "reverse" orientations (A and B) In C, the two inhibitors in the 'reverse' orientation are docked in the active site, aligning the metal binding pharmacophores with the two putative magnesium ions bound at positions D64 and D116 and D116 and E152, respectively.

References

1. Richman, D.D. (2001) *Nature*, **410** 995-1001.

2. Little, S. et. al. (2002) *N. Engl J. Med* **347**, 385-394.

3. Esposito, D., Craigie, R. (1999) *Advances in Virus Research* **52**, 319-333;

4. Asante-Appiah, E., Skalka, A. M. (1999) *Advances in Virus Res.* **52**, 351-369.

5. Hazuda, D. J., Felock, P., Witmar, M., Wolfe, A.; Stillmock, K., Grobler, J. A., Espeseth, A., Gabryelski, L, Schleif, W., Blau, C., Miller, M. D. (2000) *Science.* **287**, 646-650.

6. Wai, J. S., Egbertson, M. S., Payne, L. S., Fisher, T. E., Embrey, M. W., Tran, L. O., Melamed, J. Y., Langford, H. M., Guare, J. P. Jr., Zhuang, L., Grey, V. E., Vacca, J. P., Holloway, M. K., Naylor-Olsen, A. M., Hazuda, D. J., Felock, P. J., Wolfe, A. L., Stillmock, K. A., Schleif, W. A., Gabryelski, L. J., Young, S. D. (2000) *J. Med. Chem.* **43**, 4923-4926.

7. Espeseth, A. S., Felock, P., Wolfe, A., Witmer, M., Grobler, J., Anthony, N., Egbertson, M., Melamed, J. Y., Young, S., Hamill, T., Cole, J. L., Hazuda, D. J. (2000) *Proc. Natl. Acad. Sci. USA.* **97**, 11244-11249.

8. Grobler, J. A., Stillmock, K., Hu, B., Witmer, M., Felock, P., Espeseth, A., Wolfe, A., Egbertson, M. S., Bourgeois, M., Melamed, J. Y., Wai. J. S., Young, S. D., Vacca, J. P., Hazuda, D. J. (2002) *Proc. Natl. Acad. Sci. USA*, **99**, 6661-6666.

9. Fikkert, V., Van Maele, B., Vercammen, J., Hanston, A., Van Remoortel, B., Michiels, M., Gurnari, C., Pannecouque, C., De Maeyer, M., Engelborghs, Y., DeClerq, E., Debyser, Z., and Witvrouw, M. (2003) *J. Virol.*, **77**, 11459-11470.

10. Payne, L. S., Tran, L. O., Zhuang, L. H., Young, S. D., Egbertson, M. S., Wai, J. S., Embrey, M. W., Fisher, T. E., Guare, J. P., Langford, H. M., Melamed J. Y., Clark, D. L. (2001) *PCT Int. Appl.* 236, WO 010057A1.

11. Fujshita, T., Yoshinaga, T., Sato, A. (2000) *PCT Int. Appl.* 554, WO 003086A1.

12. Zhuang, L., Wai, J. S., Embrey, M. W., Fisher, T. E., Egbertson, M. S., Payne, L. S., Guare J. P. Jr., Vacca, J. P., Hazuda, D. J., Felock, P. J., Wolfe, A. L., Stillmock, K. A., Witmer, M. V., Moyer, G., Schleif, W. A., Gabryelski, L. J., Leonard, Y. M., Lynch, J. J. , Michaelson, S.R., and Young, S.D. (2003) *J. Med. Chem.* **46(4),** 453-456.

13. Pluymers, W., Paism, G., Pannecouque, C., Fikkert, V., Pommier, Y., Burke, T.R., De Clercq, E., Witvrouw, M., Neamati, N., and DeBeyser, Z. (2002*) Antimicorb. Agents Chemother.* **46,** 3292-3297.

14. Anthony, N. J., Gomez, R. P., Young, S. D., Egbertson, M, Wai, J. S., Zhuang, L., Embrey, M., Tran, L., Melamed, J. Y., Langford, H. M., Guare, J. P., Fisher, T. E., Jolly, S. M., Kuo, M. S., Perlow, D. S., Bennett, J. J., Funk, T. W. (2002), *PCT Int. Appl.* 97, Wo 200230931-A2.

15. Hazuda, D. J.; Felock, P.; Hastings, J. C.; Pramanik, B.; Wolfe, (1997) *J. Virol.*, **71**, 7005-7011.

16. Vacca, J. P.; Dorsey, B. D.; Schleif, W. A.; Levin, R. B.; McDaniel, S. L.; Darke, P. L.; Zugay, J.; Quintero, J. C.; Blahy, O. M.; Roth, E.; Sardana, V. V.; Schlabac, A. J.; Graham, P. I.; Condra, J. H.; Gotlib, L.; Holloway, M. K.; Lin, J.; Chen, I.-W.; Vastag, K.; Ostovic, D.; Anderson, P. S.; Emini, E. E.; Huff, J. R. (1994) *Proc. Natl. Acad. Sci. USA.* **91**, 4096-4100.

17. Butler, S. L., Hansen, M. S. T., Bushman, F. D. (2001), *Nature Med.* **7**, 631-633.

18. In-house distance geometry program was written using the theory and algorithms from: Crippen, C. M.; Havel, T. F., "Distance Geometry and Molecular Conformation", D. Bawden, Ed.; Research Studies Press, Wiley, New York, 1988 and Kuszewski, J.; Nilges, M.; Brunger, A. T. (1992) *J. of Biomolecular NMR*, 2, 33-56.

19. Halgren, T. A. (1996) *J. Comput. Chem.* **17**, 490-586; 616-641 (b) Halgren, T. A. (1996) *J. Comput. Chem.* **17**, 520-552; (c) Halgren, T. A. (1996) *J. Comput. Chem.* **17**,

553-586; (d) Halgren, T. A. and Nachbar, R. B. (1996) *J. Comput. Chem.* **17**, 587-615; (e) Halgren, T. A. (1996) *J. Comput. Chem.* **17**, 616-641.

20. Maignan, S., Guilloteau, J. P., Zhou-Liu, Q., Clement-Mella, C., Mikol, V. (1998) *J. Mol. Biol.* **282**, 359-368.

21. Young, S. D. (2001) *Current Opinion in Drug Discovery and Development* **4**, 402-410.

22. Neamati, N. (2002) *Expert Opin. Ther. Patents.* **12**, 709-724.

23. Saag, M. S., Emini, E. A., , Laskin, O. L., Douglas, J., Lapidus, W. I., Schleif, W. A., Whitley, R. J., Byrmes, V. W., Hildebrand, C., Kappes, J. C., Anderson, K. W., Massari, F. E., Shaw, G. M., and the L-697,661 Working Group. (1993) *N. Engl. J. Med.* **329**, 1065-1072.

24. Shaw-Reid, C. A., Munshi, V., Graham, P., Wolfe, A., Witmer, M., Danzeisen, R., Olsen, D. B., Carroll, S. S., Embrey, M., Wai, J. S., Miller, M. D., Cole, J. L., and Hazuda, D. J. (2003). *J Biol Chem* 278: 2777-2780.

25. Summa, V., Petrocchi, A., Pace, P., Matassa, V.G., De Francesco, R., Altamura, S., Tomei, L., Koch, U., and Neuner, P. (2004) *J. Med. Chem.* **47**, 14-17.

26. Schames, J. R.; Henchman, R. H.; Siegel, J. S.; Sotriffer, C. A.; Ni, H.; McCammon, J. A.. *J. Med. Chem.* (2004); **47**, 1879-1881.

27. Goldghur, Y., Dyda, F., Hickman, A.B., Jenkins, T.M., Craigie, R., and Davies, D.R. (1999) *Proc. Natl. Acad. Sci* **96**, 13040-13043.

28. Chen, J.C.H, Krucinski, J., Miercke, L.J.W., Finer-Moore, J.S, Tang A.H., Leavitt, A.D., and Stroud R.M. (2000) *Proc. Natl. Acad. Sci.* **97**, 8233-8238.

Figure 1.

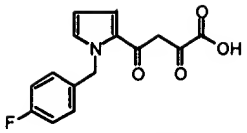

L-731,988 (1)

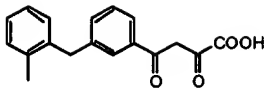

Diketo acid (2)

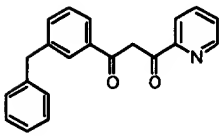

Diketone (3)

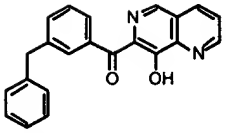

Naphthyridine ketone (4)

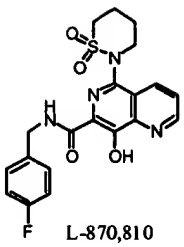

L-870,810

Figure 2.

Pharmacokinetic profile of L-870,810 after intravenous and oral administration of its sodium salt to rats and dogs.

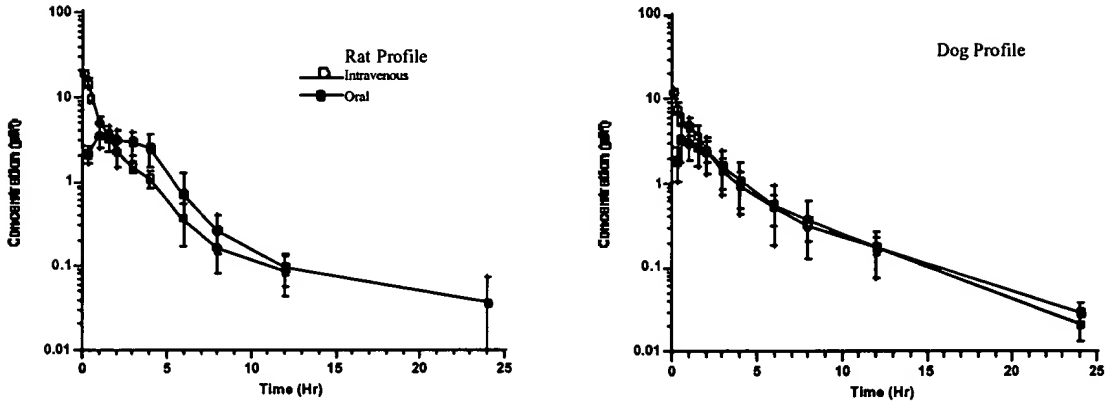

Figure 3.

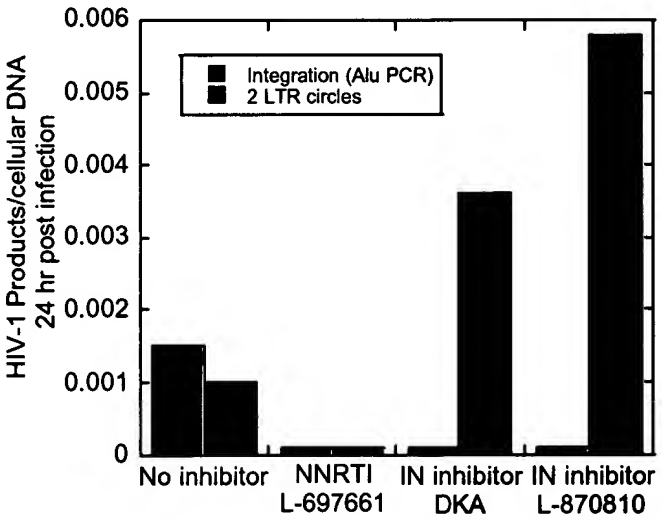

Figure 4

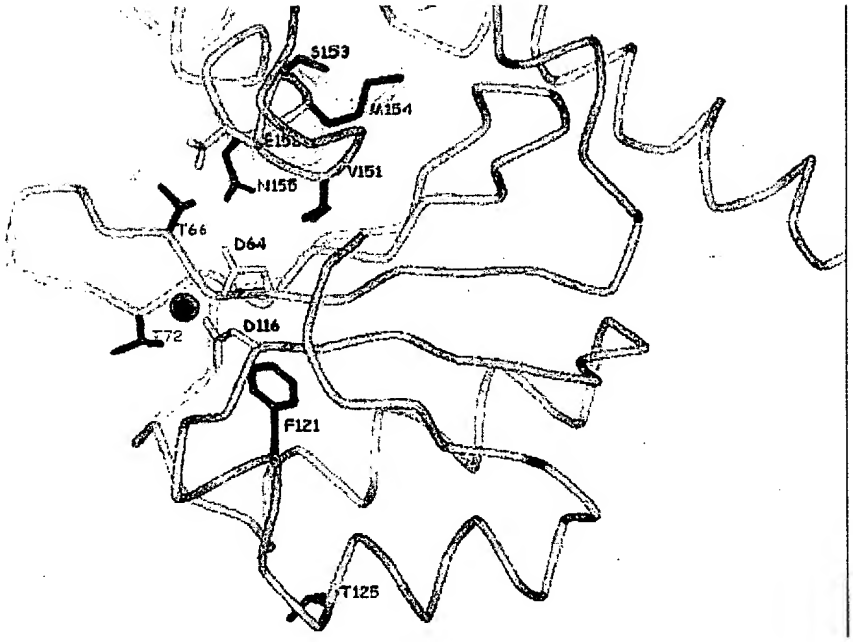

Figure 5

A. Forward

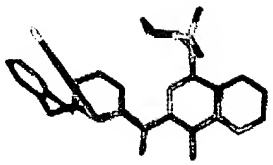

B. Reverse

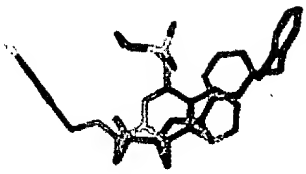

C.

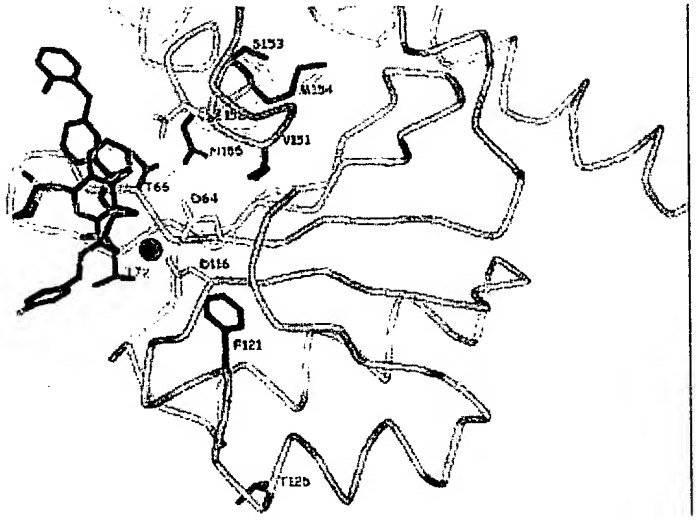

Table 1. Activity of L-870,810 and diketo acid (2) in single cycle infection assays with HIV-1 containing site directed mutations in integrase

	Diketo acid (2)	L-870,810	Sustiva
L-870,810 selected mutations			
F121Y	1X	**4X**	1X
T125K	1X	1X	1X
V151I	1X	1X	1X
F121Y/T125K	1X	**16X**	1X
V72I/F121Y/T125K	1X	**20X**	1X
V72I/F121Y/T125K/V151I	3X	**100X**	1X
Diketo acid selected mutations			
T66I	1X	2X	1X
S153Y	**4X**	1X	1X
M154I	1X	1X	1X
T66I/M154I	1X	2X	1X
T66I/S153Y	**8X**	2X	1X
N155S	**20X**	**12X**	1X

>4x = significant loss of susceptibility vs. wild type HXB2

Integrase Inhibitor Therapy and Cellular Immune Responses Mediate Sustained Antiviral Effects in Simian Immunodeficiency Virus Infection

Daria J. Hazuda[1*], Steven D. Young[2*], James P. Guare[2], Neville J. Anthony[2], Robert P. Gomez[2], John S. Wai[2], Joseph P. Vacca[2], Larry Handt[3], Sherri L. Motzel[3], Hilton J. Klein[3], Geethanjali Dornadula[1], Robert M. Danovich[1], Marc V. Witmer[1], Keith A. Wilson[4], Lynda Tussey[4], William A. Schleif[4], Lori S. Gabryelski[4], Lixia Jin[5], Michael D. Miller[1], Danilo R. Casimiro[4], Emilio A. Emini[4], and John W> Shiver[4]

*** To whom correspondence should be addressed.**
E-mail steve_young@merck.com **and** daria_hazuda@merck.com
Telephone 215-652-7204
Fax 215-652-0994

Departments of Biological Chemistry[1], Medicinal Chemistry[2], Laboratory Animal Research[3], Vaccine Research[4] and Drug Metabolism and Pharmaceutical Research Merck Research Laboratories, P.O. Box 4. West Point, PA 19486. USA.

Integrase inhibitors present an important opportunity for the development of new chemotherapeutic agents to treat HIV-1 infection. Herein we demonstrate that L-870812, a structurally novel, orally bioavailable inhibitor of HIV-1 and SIV integrase, is efficacious in rhesus macaques infected with the simian-human immunodeficiency virus (SHIV) 89.6P. When treatment is initiated prior to virus-mediated CD4 cell depletion, L-870812 monotherapy mediates a sustained suppression of viral replication, preserves CD4 cell levels and permits the induction of pronounced virus-specific cellular immune responses. L-870812 is also shown to be effective after the establishment of chronic infection, however, the magnitude and duration of the therapeutic effect is variable and correlates with the pre-existing cellular immune response. These studies demonstrate that integrase inhibitors are effective antiviral agents *in vivo* and provide evidence supporting a critical role for cellular immunity in moderating an effective response to chemotherapy in an experimental model of retroviral infection.

The substantial incidence of resistance observed in both therapy-experienced HIV-1 infected patients and newly acquired HIV-1 infections (*1-5*) underscores the need for new treatment options as well as the importance of maximizing the durability of available therapeutic regimens. Agents currently licensed for the treatment of HIV-1 disease target

two of the three virally-encoded enzymes, reverse transcriptase and protease (*6-8*). Integrase, the third HIV-1 enzyme essential for replication, is required to integrate the viral DNA into the cellular genome (reviewed in *9, 10*). Integration is a multi-step reaction that includes assembly of a stable complex with the viral DNA, 3' endonucleolytic processing of the viral DNA ends, and strand transfer or joining of the viral and cellular DNAs. Compounds that selectively inhibit strand transfer have provided proof of concept for integrase as a chemotherapeutic target for HIV-1 *in vitro* (*11*). In this investigation we have used L-870812 (*12*) (Figure 1), a novel napthyridine carboxamide inhibitor of strand transfer which has potent activity against both HIV-1 and the related simian lentivirus, SIV to study efficacy *in vivo*. The studies were designed to evaluate the effectiveness of integrase inhibitors as a new class of antiretroviral agents and to assess the contribution of immune function in chemotherapeutic intervention using rhesus macaques as an experimental model for early- and late-stage retroviral infection.

Rhesus macaques infected with SHIV 89.6P exhibit an accelerated course of disease marked by a rapid and profound depletion of circulating CD4 cells concomitant with the progression from acute viremia to a chronic phase at approximately two weeks post-infection (*13*). To evaluate the efficacy of chemotherapeutic intervention in the context of early or late disease, the current study included two infected cohorts, with six animals each. One cohort initiated therapy with L-87012 prior to virus-mediated CD4 cell depletion, near the peak of acute viremia at day 10 post-infection and were continued on monotherapy until day 87 post-infection. In the second cohort, therapy was delayed until the chronic phase was well established at day 87 and the animals were treated for 45 days. L-870812 was initiated at an oral dose of 10.0 mg/kg twice daily to achieve a twelve hour plasma concentration approximating twice the concentration required for 95% inhibition of viral replication measured in the presence of 50% rhesus monkey serum. All animals were bled twice weekly to monitor plasma viral RNA (vRNA) and CD4 cell counts. Antiviral cellular immune responses were evaluated by γ–interferon (IFN) enzyme-linked immunospot (ELISPOT), tetramer staining, and intracellular cytokine staining (ICS) analyses of peripheral blood mononuclear cells (PBMCs) against virus antigen-specific peptide pools. Resistance was also assessed by sequencing the

integrase coding region from plasma vRNA for each treated animal at every time point with detectable viral load. In addition, PBMCs from selected time points were co-cultured with uninfected CEMx174 cells in the presence or absence of 100 nM L-870812.

The viral load and CD4 cell count data for the early and delayed treatment studies are presented in Fig. 2 and Fig. 3, respectively. As anticipated for this aggressive model, the peak of acute plasma viremia occurred at approximately day 14 post-infection with a maximum titer of 10^7 to 10^9 copies of vRNA per ml of plasma. This was immediately followed by a decline in circulating vRNA and CD4 cell levels. In the delayed treatment cohort, CD4 cell counts rapidly declined to less than 100 cells/μl plasma with four animals exhibiting less than 10 cells/μl within two to three weeks post-infection (Fig 3). During the chronic phase of the infection, plasma vRNA levels ranged between 1×10^4 and 5×10^6 copies/ml, with an average viral load of 2×10^6 copies/ml.

In contrast to the delayed treatment cohort (Fig. 3), animals treated with L-870812 starting at day 10 post infection exhibited either a minimal or a transient decrease in circulating CD4 cell count which recovered and stabilized within ten days after initiating therapy (Fig 2). The animals subsequently maintained a CD4 cell count above 200 cells/μl (at day 55, average = 602, range = 261 to 1267) for the entire treatment period. In four of the six animals, viral replication was suppressed to undetectable levels (less than or equal to 0.25×10^2 vRNA copies/ml), representing a decrease in viral load of more than four orders of magnitude relative to the average of the untreated group (Fig 2). Although the remaining two animals (99-0075 and 99-0043) did not achieve undetectable suppression, they exhibited little or no decline in CD4 cell count and had average viral loads that were 10- and 100-fold lower than the average of the group untreated during this period (3×10^4 copies/ml and 1×10^5 copies/ml, respectively, versus 2×10^6 copies/ml).

In the early treatment cohort, each of the four best responders maintained a plasma level of L-870812 above 1.0 μM at 12 hours post dosing as evidenced by at least two independent determinations. In the two animals with detectable viremia, the L-870812

concentration measured at trough was 0.7 μM and 0.6 μM, respectively, suggesting suboptimal exposure may have limited the therapeutic response and/or selected drug resistant variants. In untreated animals, the integrase sequence determined at each time point was identical to that of the original challenge virus whereas a mutation in integrase at position 155 (N to H) was observed beginning on days 28 and 32 in the treated animals with detectable viremia (99-0075 and 99-0043, respectively). However, the appearance of the mutant as the predominant virus species on days 35 and 38 was not associated with a frank rebound in viral plasma levels (Fig 2) and despite incomplete suppression, there was no suggestion of an increase in vRNA levels or decline in CD4 count. In co-cultivation studies with PBMCs from both treated and untreated animals isolated on days 25, 38, 80, and 84, virus was recovered from cultures maintained in the absence of L-870812, but not when L-870812 was present. Sequencing of these viruses revealed only wild type integrase in all samples, including those derived from PBMCs isolated from 99-0075 and 99-0043 at time points where the mutant was the dominant species. The inability to rescue the N155H virus *in vitro* suggests a compromised replication phenotype may contribute to maintaining a lower viral load in these animals in the presence of continued selective pressure and is consistent with the observation that discontinuation of therapy in animal 99-0075 resulted in a 10-fold increase in viral load (Fig. 2) concomitant with reversion of the virus population to the wild type integrase sequence on day 110.

To study the effect of chemotherapy in later stage disease, L-870812 was administered starting on day 87 post-infection (Fig. 3). At therapy initiation the animals in this cohort had an average viral load of 2×10^6 copies/ml and a CD4 cell count of 35 cells/μl. Four of the six animals had a severely compromised immune status as evidenced by a CD4 cell count below 10 cells/μl. After ten days of L-870812 therapy, each of the animals exhibited a 10- to 100-fold reduction in viral load and an increase in the number of circulating CD4 cells. CD4 cell counts were increased from 3 cells/μl to 20 cells/μl within 14 days of initiating treatment with L-870812 in the most immunosuppressed animals (99-0085, 01-R023, 99-0079 and 99-0011) and from 150 cells/μl to 200 cells/μl in the least immunocompromised animal (98-0153).

While L-870812 was initially effective in this cohort, in contrast to the early treatment group, extended therapy was notably less efficacious. Moreover, both the magnitude and durability of the response to L-870812 in individual animals within the delayed treatment group (Fig 3) correlated with pretreatment viral load, CD4 cell count and cellular immune status in each subject. In animal 98-0153 which initiated therapy on day 87 with the highest CD4 count and lowest viremia, viral load was reduced by greater than 100-fold and remained below the assay limit of detection for the 45-day duration of the study. In contrast, the four animals which started therapy with the lowest CD4 cell counts and highest viral loads, exhibited a rebound in plasma viral levels within two weeks. Sequencing of the virus at multiple time points (days 105, 107, 110) during the rebound revealed only virus containing the wild-type integrase sequence (Fig. 3). The absence of any sequence change in integrase suggests the increase in viral load may have resulted from altered replication dynamics due to the greater number of target CD4 cells rather than selection for resistance. However, by day 112, i.e. 25 days after initiating therapy, animals that experienced incomplete suppression selected virus expressing the N155H mutation in integrase, although as in the early treatment cohort this was not accompanied by a rebound in viremia.

Cellular immune responses against the viral gag, nef and tat proteins were evaluated in all animals starting on day 12 post infection and at 2 week intervals. As shown in Table 1, the striking differences in the both the magnitude and sustained nature of the chemotherapeutic response observed between the early and delayed treatment groups was also associated with significant differences in their respective viral specific immune responses. L-870812 therapy initiated during early infection preserved the CD4 cell counts and permitted the induction of noted, persistent SHIV specific cellular immunity. Significantly stronger responses against gag and nef proteins were observed in the early-treated cohort compared to the group untreated during this period and were evident as early as day 25 post infection (gag, $p < 0.033$; nef, $p < 4 \times 10^{-5}$). These responses involved both $CD8^+$ and $CD4^+$ T-cells (Table 1). This immune response likely contributed to the robust antiviral responses observed during L-870812 treatment and to the continued

control of virus replication after the discontinuation of therapy in the early treatment group (Fig. 2). Neutralizing antibody responses against the infecting virus were minimal throughout the experimental period (data not shown).

In the delayed treatment group, initiation of L-870812 therapy did not result in either the induction of or increase in cellular immune responses (data not shown). However, the two animals (01-R017 and 98-1053) that expressed the best virological outcomes both before and during L-870812 therapy, exhibited SHIV specific cellular immune responses prior to initiating therapy. In addition, the magnitude of the L-870812 chemotherapeutic effect correlated with the cellular immune status (Fig. 3 and Table 1). Animal 98-0153 which initiated therapy with the highest CD4 cell count (150 cells/μl) and SHIV specific cellular immune response was the only animal in the delayed treatment cohort to achieve and maintain viral load suppression to levels below 10^2 copies/ml. In contrast, the four animals in this cohort (99-0111, 99-0079, 99-0085 and 01-R023) which did not develop significant virus specific cellular immunity also exhibited the least effective response to therapy. The correlation of the therapeutic response between the two cohorts and among animals within the delayed treatment group with cellular immune function suggests the control of viremia mediated by an chemotherapy agent such as the integrase inhibitor, L-870,812, is significantly facilitated by viral specific cellular immunity.

Integrase inhibitors represent a promising new class of agents for treating HIV-1 infection both in treatment-naïve patients and patients harboring viruses resistant to current therapies. L-870812 represents a potent prototype of a new structural class of integrase strand-transfer inhibitors, the napthyridine carboxamides. The antiviral activity of L-870812 in SHIV-89.6P infected rhesus macaques, when administered as monotherapy, provides the first demonstration of the *in vivo* biological activity of integrase inhibitors and demonstrates that such compounds can be engineered with the appropriate potency and pharmacokinetic properties necessary to achieve efficacy in HIV-1 infected patients. These studies were conducted over the course of several months to permit the systematic evaluation of resistance to this novel class of agents *in vivo* and

to explore the relationship between antiretroviral therapy and cellular immune function by administering therapy either early or late in infection.

As monotherapy, L-870812 was able to elicit a 10 to >100 fold decrease in viral load and positively affect on CD4 cell count both in animals treated early or late in infection. Although chronic administration of L-870812 in animals with incomplete viral suppression led to the selection of a mutation in integrase, N155H, the animals maintained an overall lower viral load and there was no decline in CD4 cell counts despite ongoing replication. The mutant viruses could not be rescued and when engineered into HIV-1, the N155H mutation engendered a thirty-fold loss of susceptibility to L-870812 that was accompanied by a defect in viral replication capacity (<30% specific infectivity relative to the wild-type HIV-1 as measured in a single cycle infection assay, Witmer and Hazuda, unpublished). Mutations at 155 as well as other active site residues including 151, 153 and 154 have been observed in *in vitro* selection studies with diketo acid analogs and also noted to reduce both integrase enzymatic function and viral replication capacity (*11, 14*). While these data are encouraging and suggest L-870812 and related integrase inhibitors may select for viruses with reduced pathogenicity, it is possible that continued replication would eventually lead to the selection of compensatory mutations that could not be observed within the time frame of the current study (months).

Although L-870812 was effective in both the early and delayed treatment models, the activity of L-870812 was most robust when therapy was started early in infection. This observation is consistent with studies of human acute seroconverters suggesting that chemotherapy is also most effective in early HIV-1 disease (*15*). The overall response to L-870812 in animals initiating therapy later in infection was also notably affected by both pre-existing viral load and immune status. Together, these results demonstrate that cellular immunity plays a critical role in maximizing both the magnitude and durability of antiretroviral chemotherapy. These observations thus provide evidence in support of revisiting more aggressive intervention strategies for treating HIV-1 infection as agents with improved tolerability and convenience are introduced into clinical practice and

suggest vaccines designed to provoke a more effective HIV-1 specific cellular immune response could provide an important adjunct to enhance and sustain antiviral efficacy in HIV-1 infected patients.

Acknowledgements: We appreciate the technical support of Peter Felock, Kara Stillmock, Anthony Carella, Gregory Moyer, Randy Newton. Peter Sczerba, Patti Reebeck, Marc Washington and Karen Wright.

Figure Legends

Figure 1. Structure and activity of L-870812

Figure 2: CD4 cell counts (blue) and viral loads (black) in SHIV-infected rhesus macaques, treated with L-870812 starting at day 10 post-infection. Individual animal data are plotted in each panel. Treatment with the integrase inhibitor continued until day 87 and animals were followed out to day 132. Results of the integrase sequence determinations in the treated animals with measurable viral loads are presented as colored symbols (black = wild type integrase, yellow = mixture of wild type and N155H integrase, red = N155H integrase)

Figure 3. CD4 cell counts (blue) and viral loads (black) in SHIV-infected rhesus macaques following the initiation of L-870812 therapy on day 87 post-infection. Results of integrase sequence determinations are presented as colored symbols (black = wild type integrase, yellow = mixture of wild type and N155H integrase, red = N155H integrase)

Figure 1

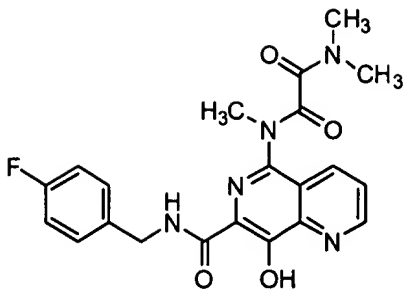

L-870812

Integrase Strand Transfer Activity:	**IC_{50} = 0.040 μM**
Antiviral Activity (10% FBS)	**IC_{95} = 0.103 μM**
(50% Rhesus Serum)	**IC_{95} = 0.350 μM**
(50% Human Serum)	**IC_{95} = 0.250 μM**
Oral Bioavailability (Rhesus)	**64%**
Half Life	**5 h**

Figure 2

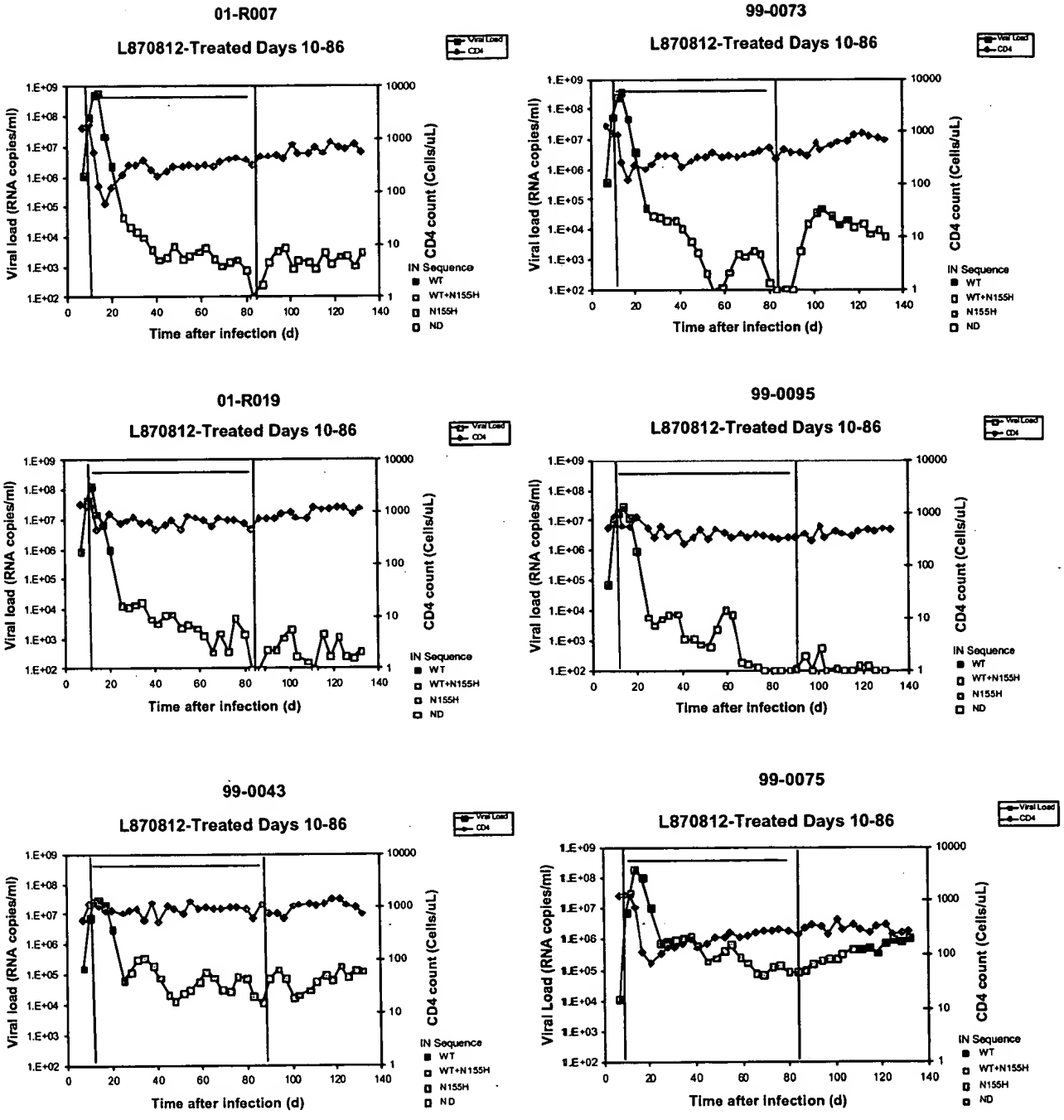
01-R007
L870812-Treated Days 10-86
99-0073
L870812-Treated Days 10-86
01-R019
L870812-Treated Days 10-86
99-0095
L870812-Treated Days 10-86
99-0043
L870812-Treated Days 10-86
99-0075
L870812-Treated Days 10-86
Viral load (RNA copies/ml)
CD4 count (Cells/uL)
Time after infection (d)
IN Sequence
WT
WT+N155H
N155H
ND

Figure 3

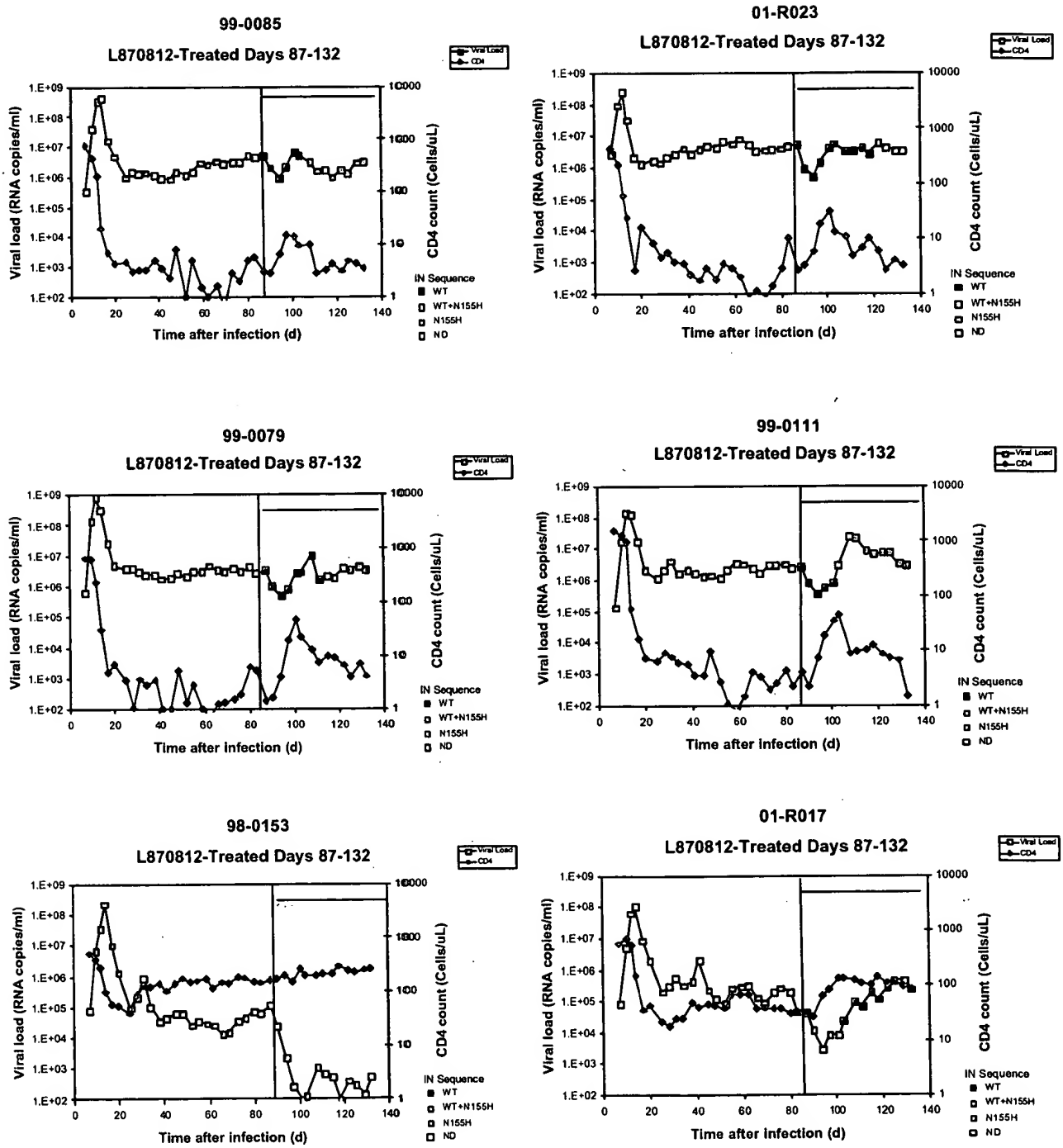
99-0085
L870812-Treated Days 87-132
01-R023
L870812-Treated Days 87-132
99-0079
L870812-Treated Days 87-132
99-0111
L870812-Treated Days 87-132
98-0153
L870812-Treated Days 87-132
01-R017
L870812-Treated Days 87-132
Viral Load
CD4
Viral load (RNA copies/ml)
CD4 count (Cells/uL)
Time after infection (d)
IN Sequence
WT
WT+N155H
N155H
ND

Table 1. Antiviral Cellular Immune Responses in SHIV-Infected Monkeys

Animal #	γ-IFN ELISPOT[a]		γ-IFN ICS[b]				CM9 Tetramer Levels[c]
			Gag		Nef		
	Gag	Nef	$CD3^+CD8^+$	$CD3^+CD4^+$	$CD3^+CD8^+$	$CD3^+CD4^+$	
L-870812-treated							
01-R019	*64*	*155*	0	173	0	233	ND
01-R007	48	*258*	362	129	170	126	ND
99-0043	*394*	*429*	*887*	*679*	45	*2176*	ND
99-0073	*1176*	*1263*	*1083*	*319*	*677*	*357*	1.93%
99-0095	*361*	*601*	*416*	*482*	0	262	ND
99-0075	*1203*	*440*	*3227*	*614*	0	*421*	2.22%
Untreated control							
01-R017	*76*	34	23	20	95	149	ND
99-0111	1	33	50	0	58	4	ND
98-0153	*753*	*621*	*1729*	*312*	64	120	1.69%
99-0079	3	*81*	0	0	160	113	ND
99-0085	30	*156*	*336*	0	183	52	0.22%
01-R023	20	18	36	0	0	160	ND

[a] Determinations were made using PBMC samples collected on day 41 post-infection. Values are reported as the mock-corrected numbers of γ-IFN spot-forming cells (SFC) per million PBMC (see Methods). Responses were individually measured against the complete gag and nef peptide pools. Positive responses are italicized as being >50 SFC per million PBMC and at least 4-fold above mock levels. No responses to the viral tat protein were noted in any of the animals. Differences between both groups in terms of nef- and gag-specific responses have associated p values < 0.0159 and 0.0411, respectively, using ANOVA single factor analyses of the log values.

[b] PBMC collected at day 52 post infection were analyzed via γ-IFN ICS method. Mock-corrected values are reported individually for the number of $CD3^+CD8^+$ or $CD3^+CD4^+$ cells per million lymphocytes. Positive responses to a pool are italicized as being >300 per million lymphocytes and being 3-fold above mock levels (see Methods). Cohort differences in the levels of $CD4^+$-type responses to gag and nef were statistically significant (p < 0.0017 and 0.0309, respectively).

Methods

Animals. All treatment and care of rhesus monkeys *(Macaca mulatta*) were in accordance with the institutional animal care protocols of Merck Research Laboratories (West Point, PA). Monkeys were analyzed for *Mamu*-A*01 allele expression according to PCR-SSP methods as described previously (*16*). Animals that were positive by the PCR reaction were subsequently confirmed by DNA sequencing of the amplified region. Animals were given intravenously with 50 monkey infectious doses (50 MID50) of cell free SHIV-89.6P (*13*). In the early intervention study, the animals initiated therapy on day 10 and were dosed twice daily with 10 mg/kg L-870812 as a suspension in methyl cellulose for four weeks, i.e., a time that was experimentally determined to achieve a sustained antiviral affect in the animals (see below) and then switched to a 20.0 mg/kg once daily dose for convenience. Monkeys were monitored for clinical signs of disease progression and cared for under the guidelines provided by the NIH "Guide for the Care and Use of Laboratory Animals".

Viral load determinations. Plasma viral RNA was measured using real-time quantitative PCR (*17*).Viral RNA purified from macaque plasma with a QiaAmp Viral RNA kit was quantified using an ABI 7900 genetic analyzer and TaqMan Gold RT-PCR reagents and the following SIV-specific oligonucleotides (0.2μM each): GAG FOR primer 5'-CTGCGTCATCTGGTGCATTC-3'; GAG REV primer 5'-CTAGGTGTCTCTGCACTATCTGTTTTG-3'; GAG probe 5'-(5/6-FAM)-CGCAGAAGAGAAAGTGAAACACACTGAGGA-(3/6TAMNph)-3'. vRNA levels were determined by comparison to a standard curve generated using RNA standards made by *in vitro* transcription from a plasmid encoding SIV gag.

In a subset of animals vRNA levels were also determined using a modified version of the ROCHE UltraSensitive Amplicor assay refereed to as 'SIV UltraSensitive Real-Time PCR Assay.' (Consolidated Laboratory Services, Van Nuys , CA) The assay has a detection limit of approximately 25 copies vRNA per mL.

ELISPOT and ICS. Interferon-γ ELISPOT assays were conducted to assay for antigen-specific T cells in monkey PBMCs following a protocol described earlier with some minor modifications (*18*). Modifications included the use of 96-well Multiscreen-IP white plates (Millipore) instead of the clear-bottom plates provided in the UCytech monkey IFN-γ ELIPSOT kit. Pools of 20-aa peptides with 10-aa overlaps and that encompass the entire sequence of SIVmac239 gag, nef, or HIV-1 tat were used at 4 μg/mL concentration per peptide to stimulate for antigen-specific responses from PBMC. Method for ICS analyses have been described elsewhere (*19*) and used with some modifications. These alterations include the following items. First, anti-hCD28 (clone L293, Becton-Dickinson) and anti-hCD49d (clone L25, Becton-Dickinson) monoclonal antibodies were added to a final concentration of 1 μg/mL to a tube containing 2 x 10^6 PBMC in 1 mL complete RPMI media. 10 μL of the peptide pool (at 0.4 mg/mL per peptide) or DMSO was added for antigen-specific or mock stimulation, respectively. Secondly, brefeldin A (Sigma) was added at a final concentration of 100 μg/mL and the cells were incubated for 16 hr at 37 °C, 5% CO_2, 90% humidity. Thirdly, cells were

stained using the following fluorescent-tagged mAbs: 20 μL per tube anti-hCD3-APC, clone FN-18 (Biosource); 20 μL anti-hCD8-PerCP, clone SK1 (Becton Dickinson); 20 μL anti-hCD4-PE, clone SK3 (Becton Dickinson); and 0.1 μg of FITC-anti-hIFN-γ, clone MD-1 (Biosource).

Analysis of resistance; integrase sequencing and cocultivation. Virus was isolated from phytohemagglutinin-activated macaque PBMCs by coculture with CEMx174 cells essentially as described (*20*). Cocultures of PBMCs isolated from L-870812-treated animals were performed in the presence and absence of L-870812 at 100nM, roughly equivalent to the IC95 of this compound for inhibition of SHIV89.6P replication in macaque PBMCs in 10%FBS. Viral growth was monitored using an SIV p27-specific ELISA according to the manufacturer's instructions (Coulter). Viral RNA was purified with a QiaAmp kit and the integrase coding region sequenced on both strand using standard methods.

References

1. S. J. Little *et al.*, *N. Engl. J. Med.* **347**, 385 (2002).
2. F. J. Palella, Jr. *et al.*, *N. Engl. J. Med.* **338**, 853 (1998).
3. G. M. Lucas, R. E. Chaisson, R. D. Moore, *Ann. Intern. Med.* **131**, 81 (1999).
4. S. Yerly *et al.*, *Lancet* **354**, 729 (1999).
5. M. R. Furtado *et al.*, *N. Engl. J. Med.* **340**, 1614 (1999).
6. M. Hogberg, I. Morrison, *Exp Opin Ther Patents* **10**, 1189 (2000).
7. H. Jonckheere, J. Anne, E. De Clercq, *Med. Res. Rev.* **20**, 129 (2000).
8. F. Lebon, M. Ledecq, *Curr. Med. Chem.* **7**, 455 (2000).
9. D. Esposito, R. Craigie, *Adv. Virus Res.* **52**, 319 (1999).
10. E. Asante-Appiah, A. M. Skalka, *Adv. Virus Res.* **52**, 351 (1999).
11. D. J. Hazuda *et al.*, *Science* **287**, 646 (2000).
12. N. J. Anthony *et al.*, in *PCT Patent Appl. WO 0230931-A2.* (2002).
13. K. A. Reimann *et al.*, *J. Virol.* **70**, 6922 (1996).
14. V. Fikkert *et al.*, *J. Virol.* **77**, 11459 (Nov, 2003).
15. R. E. Chaisson, J. C. Keruly, R. D. Moore, *JAMA* **284**, 3128 (Dec 27, 2000).
16. L. A. Knapp, E. Lehmann, M. S. Piekarczyk, J. A. Urvater, D. I. Watkins, *Tissue Antigens* **50**, 657 (1997).
17. C. A. Heid, J. Stevens, K. J. Livak, P. M. Williams, *Genome Res.* **6**, 986 (1996).
18. T. M. Allen *et al.*, *J. Virol.* **75**, 738 (2001).
19. B. R. Mothe *et al.*, *J. Immunol.* **169**, 210 (2002).
20. B. L. Lohman, J. Higgins, M. L. Marthas, P. A. Marx, N. C. Pedersen, *J. Clin. Microbiol.* **29**, 2187 (1991).